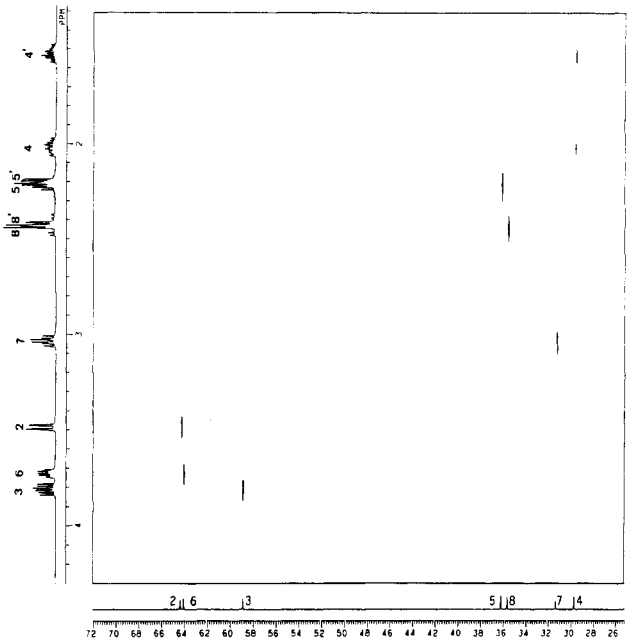

Figure 4. Contour plot of the $^{13}C-^{1}H$ chemical shift correlation spectrum of complex **10**.

are listed in Table IV. The formation of (cyclooctadienone)ruthenium(0) complex **10** strongly suggests that the nucleophilic attack of superoxide also occurred at the terminal position, C_3, of the allylic moiety of C_8H_{11} ligand.

The formation of **11** would reasonably be elucidated by the nucleophilic attack of $CHCl_2^-$ on the coordinated benzene. In this reaction, superoxide would act as a base[25] and abstract a proton from dichloromethane to generate $CHCl_2^-$.

Treatment of **4** in dichloromethane in the presence of KOH demonstrates the nucleophilic attack of $CHCl_2^-$ on the coordinated benzene, forming **11** (eq 9).

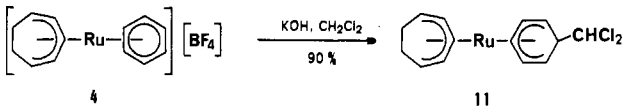

4 11 (9)

Additional investigations of the detailed mechanism of the formation of the cyclic ketone complexes are under way.

Acknowledgment. We thank Dr. T. Ikariya and Nippon Denshi Co. Ltd. for collecting NMR data with the JEOL GX-400. Financial support for this work was generously provided in part by a grant from the Ministry of Education, Science and Culture of the Japanese Government (No. 58470071).

Registry No. **1**, 91753-79-6; **2**, 103438-20-6; **3**, 103438-22-8; **4**, 103438-24-0; **5**, 103438-26-2; **6**, 103438-27-3; **7**, 103438-29-5; **8**, 103438-30-8; **9**, 103438-31-9; **10**, 103438-32-0; **11**, 103438-33-1; $[(\eta^6\text{-}C_6H_6)RuCl_2]_2$, 37366-09-9; $[(\eta^5\text{-}C_5Me_5)RuCl_2]$, 92390-47-1; $K[C_5(CO_2CH_3)_5]$, 16691-64-8.

(25) Frimer, A. A. In *The Chemistry of Peroxide*; Patai, S., Ed.; Wiley: Chichester, U. K., 1983; Chapter 14 and references cited therein.

Contribution from the Science Research Laboratory, 3M Central Research Laboratories, St. Paul, Minnesota 55144, and Department of Chemistry, University of Minnesota, Minneapolis, Minnesota 55455

Protonation of Iron, Ruthenium, and Osmium Hydrides with Fluorocarbon Acids. Stereochemical Rigidity in Seven-Coordinate $[(Ph_3P)_4OsH_3]^+[HC(SO_2CF_3)_2]^-$

A. R. Siedle,*† R. A. Newmark,† and L. H. Pignolet‡

Received November 26, 1985

The fluorocarbon acid $H_2C(SO_2CF_3)_2$ has been used to effect protonation of a series of iron, ruthenium, and osmium hydrides. The salts $[(Ph_3P)_3MH(CO)]^+[HC(SO_2CF_3)_2]^-$ (M = Ru, Os) and $[(Ph_3P)_3RuH(CO)]^+[HC(SO_2C_8F_{17})_2]^-$ were prepared from $(Ph_3P)_3MH_2(CO)$ whereas $(Ph_3P)_3Ru(CO)HCl$ yields binuclear $[(Ph_3P)_4Ru_2(CO)_2(\mu\text{-}Cl)_2(\mu\text{-}H)][HC(SO_2CF_3)_2]$. Protonation of $(diphos)_2FeHCl$ and $(diphos)_2FeH_2$ yields $[(diphos)_2FeCl][HC(SO_2CF_3)_2]$ and $[(diphos)_2Fe(\eta^2\text{-}H_2)H][HC(SO_2CF_3)_2]$, respectively. The latter reacts with $(CH_3)_3P$ to form $[(diphos)_2FeHP(CH_3)_3][HC(SO_2CF_3)_2]$. Protonation of the polyhydride $(Ph_3P)_3OsH_4$ in the presence of Ph_3P produces $[(Ph_3P)_4OsH_3][HC(SO_2CF_3)_2]$, whose crystal structure [at −90 °C; $P2_1/n$, a = 14.122 (6) Å, b = 13.636 (1) Å, c = 33.646 (2) Å, β = 90.90 (4)°, Z = 4, R = 0.095] indicates that in it osmium has a distorted, capped octahedral coordination geometry. The cation is stereochemically nonrigid at ≥−80 °C. $\Delta H^{\ddagger}$ and $\Delta S^{\ddagger}$ for the fluxional process, determined by ^{31}P DNMR, are 5.3 ± 0.3 kcal/mol and −16 ± 1 eu.

Introduction

We have previously reported that the fluorocarbon acids **1–3** are useful reagents for the synthesis of novel cationic compounds formed by the protonation of organometallic hydrides and carbonyl hydrides.[1-4] This is because **1–3** are strong, nonoxidizing acids

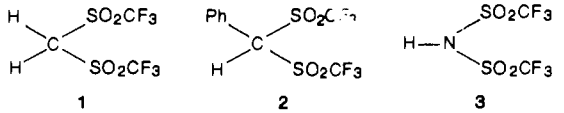

1 **2** **3**

that, upon proton transfer, form noncoordinating conjugate bases. The bis(trifluoromethylsulfonyl)alkanes **1** and **2** and their higher perfluoroalkyl homologues are nonhygroscopic and may be easily manipulated in air in anhydrous form; **1**, after prolonged exposure to the atmosphere, contains 0.02% water determined by Karl Fischer analysis. Since these fluorocarbon acids are soluble in nondonor solvents such as toluene and dichloromethane, they may be used to study the proton-transfer chemistry of organometallic coordination compounds with minimal or no interference from strong interactions involving electron transfer, adventitious water,

† 3M Central Research Laboratories.
‡ University of Minnesota.

(1) Siedle, A. R.; Newmark, R. A.; Pignolet, L. H.; Howells, R. D. *J. Am. Chem. Soc.* **1984**, *106*, 1510.
(2) Siedle, A. R.; Newmark, R. A.; Pignolet, L. H. *Organometallics* **1984**, *3*, 855.
(3) Siedle, A. R.; Newmark, R. A.; Pignolet, L. H.; Wang, D. X.; Albright, T. A. *Organometallics* **1986**, *5*, 38.
(4) Siedle, A. R.; Newmark, R. A.; Gleason, W. B. *J. Am. Chem. Soc.* **1986**, *108*, 767.

0020-1669/86/1325-3412$01.50/0

donor solvents, or the conjugate bases. Here, we report a survey of the protonation chemistry of some hydrides of iron, ruthenium, and osmium and describe the structure and dynamic properties of the cynosure of this paper, $[(Ph_3P)_4OsH_3]^+[HC(SO_2CF_3)_2]^-$, a seven-coordinate osmium hydride in which a rapid rearrangement process is significantly slowed at low temperatures. Generally, the reactivity pattern exhibited by phosphine-substituted group VIII hydrides and carbonyl hydrides is proton-transfer followed by reductive elimination of dihydrogen.

Results and Discussion

Because efforts to obtain anions that are noncoordinating under all circumstances have been incompletely unsuccessful,[5] we begin by outlining criteria by which the $HC(SO_2CF_3)_2^-$ ion (and its congeners) may be judged to be noncoordinating. Nuclear magnetic resonance data are generally most useful and, because of the good solubility of $H_2C(SO_2CF_3)_2$ derivatives in dichloromethane, are usually obtained in CD_2Cl_2. In salts containing ionic $HC(SO_2CF_3)_2^-$, the ^1H and ^{19}F NMR spectra reveal sharp resonances at 3.7 and −81 ppm, respectively. In crystallographically characterized *trans*-$(Ph_3P)_2PtH[C\text{–}HC(SO_2CF_3)_2]$, in which the fluorocarbon ligand is bonded to platinum through the central, methine carbon atom, the corresponding resonances shift to 5.0 and −77 ppm.[4,6] Hybridization at the methine carbon is approximately sp^3 in $H_2C(SO_2CF_3)_2$ and $(Ph_3P)_2PtH[C\text{–}HC(SO_2CF_3)_2]$, and reflecting this, the methine C–H coupling constants are 144 and 148 Hz, respectively. In the anion $HC(SO_2CF_3)_2^-$, hybridization is more nearly sp^2,[7] and in its NH_4^+ salt, J_{CH} is 186 Hz. Thus, the magnitude of the C–H coupling constants provide an additional probe of potential bonding to carbon in $HC(SO_2CF_3)_2$ derivatives. ^{13}C NMR spectra of such compounds are usually obtained in aromatic solvents such as toluene since there is close overlap between solvent resonances in chlorinated hydrocarbons and the methine ^{13}C signal of interest. For this purpose, the $HC(SO_2C_8F_{17})_2$ derivatives are especially useful; the long-chain perfluoroalkyl groups are quite effective in imparting to fluorocarbon acid salts high solubility (0.2–0.4 M) in aromatic hydrocarbons although extensive ion pairing may well occur in such solvents.

No well-defined example of metal coordination to oxygen in the $HC(SO_2CF_3)_2$ group has yet been obtained. In the compounds reported in this paper, coordination to only one oxygen atom should considerably perturb the fluorine electron density on one of the CF_3 groups and this mode of bonding is excluded on the basis of observation of chemically equivalent CF_3 groups at −81 ppm. Furthermore, coordination to oxygen would also be expected to shift the frequencies of the S–O bands in the infrared spectrum relative to, e.g., the NH_4^+ salt and this is not observed.

The anion $HC(SO_2CF_3)_2^-$ may also be discerned by conductance measurements; its salts behave as 1:1 electrolytes in dichloromethane. Thus, for example, the conductance of 1.3×10^{-3} M solutions of $[(n\text{-}C_3H_7)_4N]^+[HC(SO_2CF_3)_2]^-$ and $[(n\text{-}C_3H_7)_4N]^+[N(SO_2CF_3)_2]^-$ in dichloromethane are 30 and 32 Ω^{-1} cm^2 mol^{-1}, respectively, while that of $(Ph_3P)_2PtH[C\text{–}HC(SO_2CF_3)_2]$ is 6 Ω^{-1} cm^2 mol^{-1}.

When toluene solutions of $(Ph_3P)_3MH_2(CO)$ [M = Ru, **4**; M = Os, **5**] and equimolar amounts of $H_2C(SO_2CF_3)_2$ are stirred at 30 °C, the crystalline solvates $[(Ph_3P)_3RuH(CO)]^+[HC(SO_2CF_3)_2]^-\cdot 2C_7H_8$ (**6**) and $[(Ph_3P)_3OsH(CO)]^+[HC(SO_2CF_3)_2]^-\cdot 2C_7H_8$ (**7**) separate in 73 and 82% yields, respectively. The cationic ruthenium hydride derivative **6** exhibits ν_{RuH} at 1995 cm^{-1} (m) and ν_{CO} at 1945 cm^{-1} (s). In **7**, the Os–H and Os–CO bands occur at 2065 (m) and 1935 (s) cm^{-1}, respectively. The high-field portion of the ^1H NMR spectrum of **6** displays a doublet of triplets at δ −7.4 with J_{HP}(trans) = 100 Hz (d) J_{HP}(cis) = 25 Hz (t); in **7**, the OsH proton has δ −7.0 with J_{PH}(trans) = 82 Hz (d) and J_{PH}(cis) = 25 Hz; the spectra of both compounds contain singlets at 3.7 ppm due, as are the ^{19}F resonances at −81.4 ppm, to $HC(SO_2CF_3)_2^-$. The ^{31}P NMR spectrum of **7** reveals a doublet of doublets of relative area 2 at δ 17.0 (J_{PP} = 10.7 Hz, J_{PH} = 25 Hz) and an unresolved multiplet of unit area at δ 4.5. Similarly, the ^{31}P spectrum of **6** contains two resonances at δ 42.8 (2P) and 21.6 (1P), but in this case, P–P coupling in the A_2BX pattern is not well resolved. These data are most plausibly accommodated by square-pyramidal structures for **6** and **7** having three basal Ph_3P groups and an apical CO ligand, and indeed, square-pyramidal geometries are most often adopted by d^6 ruthenium.[8]

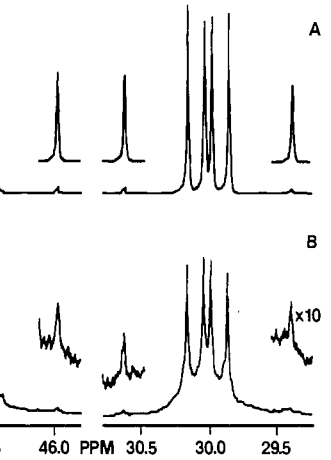

Figure 1. Calculated (A) and experimental (B) $^{13}P\{^1H\}$ spectra of $[(Ph_3P)_4Ru_2(CO)_2(\mu\text{-}Cl)_2(\mu\text{-}H)][BPh_4]$.

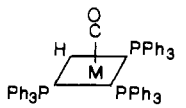

However, an alternate trigonal-bipyramidal geometry with a Ph_3P group and a hydride in axial positions cannot be ruled out from NMR data since the SP and TBP isomers both have C_{2v} symmetry.

That the $HC(SO_2CF_3)_2^-$ ion in **6** is not coordinated through oxygen to ruthenium is indicated by its infrared spectrum, which shows S–O stretching bands at 1330 and 1095 cm^{-1}, essentially unchanged from the 1330- and 1085-cm^{-1} absorptions in the piperidinium salt of $HC(SO_2CF_3)_2^-$. The ^{13}C NMR spectrum of $[(Ph_3P)_3RuH(CO)]^+[HC(SO_2C_8F_{17})_2]^-$ (**6a**) in C_6D_6 discloses a methine carbon resonance at δ 64.2 with J_{CH} = 184 Hz, consistent with an ionic formulation. This is supported by the conductance of a 1×10^{-3} M solution of **6** in dichloromethane that is 30 Ω^{-1} cm^2 mol^{-1}.

The reaction of $(Ph_3P)_3RuHCl(CO)$ with **1** or **2** provides an example of cluster formation associated with protonation. It yields $[(Ph_3P)_4Ru_2(CO)_2(\mu\text{-}Cl)_2(\mu\text{-}H)]^+[HC(SO_2CF_3)_2]^-$, purified as the tetraphenylborate salt **8**, ν_{CO} 1975 cm^{-1}. The high-field portion of the ^1H NMR spectrum of **8** shows a triplet of triplets of unit area at δ −13.2 with J_{PH}(trans) = 43.0 and J_{PH}(cis) = 10.6 Hz. The $^{31}P\{^1H\}$ NMR spectrum reveals two multiplets of equal area at 30.0 and 46.6 ppm (cf. Figure 1). When only the aromatic protons are spin-decoupled, the downfield resonance splits into two multiplets separated by ca. 44 Hz, indicating that the larger P–H coupling involves the ^{31}P nuclei with δ 46.6. These data establish that **8** contains one bridging hydride which is coupled

(5) Recent examples include $Me_2PhP(CO)_3(NO)W(\mu\text{-}F)SBF_5$ (Hersh, W. H. *J. Am. Chem. Soc.* **1985**, *107*, 4599), $(C_5Me_5)(CO)_2FeOSO_2CF_3$ (Humphrey, M. B.; Lamanna, W. M.; Brookhart, M.; Husk, G. R. *Inorg. Chem.* **1983**, *22*, 3355), $AuMe_2(H_2O)OSO_2CF_3$ (Komiya, S.; Huffman, J. C.; Kochi, J. K. *Inorg. Chem.* **1977**, *16*, 2138), $Pd(NR_2C_2H_4CO)(R_2NH)(OSO_2CF_3)$ (Anderson, O. P.; Packard, A. B. *Inorg. Chem.* **1979**, *18*, 1129), and $(CO)_5M(O_3SCF_3)$ (M = Mn, Re) (Nitschke, J.; Schmidt, S. P.; Trogler, W. C. *Inorg. Chem.* **1985**, *24*, 1972).

(6) Siedle, A. R.; Gleason, W. B.; Newmark, R. A., manuscript in preparation. In this particularly favorable case, long-range spin coupling between ^{195}Pt and the methine ^1H and ^{13}C nuclei as well as ^{19}F is observable.

(7) This follows from the 126 (1)° S–C–S angle in the Rb^+ salt: Davoy, K.; Gramstad, T.; Huseby, S. *Acta. Chem. Scand., Ser. A* **1979**, *33A*, 359.

(8) Hoffman, P. R.; Caulton, K. G. *J. Am. Chem. Soc.* **1975**, *97*, 4221.

to two chemically equivalent trans phosphines with J_{PH}(trans) = 43.0 Hz and also to two chemically equivalent phosphines with J_{PH}(cis) = 10.6 Hz. The ^{31}P multiplets are typical of an AA'XX' pattern, exact analysis[9] of which reveals J(AA') = 47.6, J(AX) = 22.5, J(AX') = 1.6, and J(XX') = 0 Hz. The root-mean-square error between calculated (cf. Figure 1) and observed transition frequencies is 0.1 Hz. The 43.0-Hz triplet observed in the ^{1}H spectrum requires that the chemically equivalent A and A' ^{31}P nuclei be trans to the hydride and that they are on different ruthenium atoms. These data suggest that **8** is binuclear, having one bridging hydride and two bridging chloride ligands so as to give the quotidian[10] face-shared bioctahedral coordination geometry. Although doublets would be expected in the ^{31}P{^{1}H}

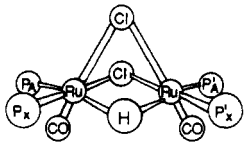

8

spectrum for an AX spin system comprising two different phosphine ligands (one cis and one trans to hydride) on each ruthenium atom, multiplets are observed due to three-bond P–P coupling that renders the phosphines magnetically inequivalent. It is known that ^3J(PRuRuP) coupling in confacial bioctahedral Ru(II) is a sensitive function of the nature of the bridging ligand(s) X and the PRu–X–RuP angle.[11-13] For example, first-order analysis of the ^{31}P NMR spectrum of $[(p\text{-tol})_3P]_4Ru_2H_4Cl_2$ (p-tol = p-tolyl) indicates that ^3J(PRuRuP) couplings are 40, 4, and 0 Hz for bond angles, calculated as the sum of the P–Ru–P and Ru–Ru–P angles, of 288, 258, and 239°, respectively. These coupling constants are, in fact, quite similar to those found in **8**. Since ^3J(PRuRuP) is dependent on the deviation of the PRuRuP angle from linearity, the bridging bond angles in **8** are probably similar to those in $[(p\text{-tol})_3P]_4Ru_2H_4Cl_2$, which contains two μ-Cl ligands and one μ-H ligand. The hydride in **8** appears not to be acidic since no reaction with proton sponge [1,8-bis(dimethylamino)-naphthalene] in CD_2Cl_2 was observed at room temperature.

Protonation of $(diphos)_2FeHCl$ in toluene with **1** produces $[(diphos)_2FeCl]^+[HC(SO_2CF_3)_2]^-$ (**9**). The ^{31}P NMR spectrum of this salt is temperature-invariant between −90 and −30 °C and displays two broad ($w/2$ = 30 Hz) peaks at 93.4 and 80.3 ppm, which convey little stereochemical information, and the line width obscures observation of P–P coupling; no hydride resonance is apparent in the ^{1}H NMR spectrum, which argues against a $(diphos)_2FeH_2Cl^+$ formulation (vide infra). A similar reaction of $(diphos)_2FeH_2$ and $H_2C(SO_2CF_3)_2$ yields $[(diphos)_2Fe(\eta^2\text{-}H_2)H]^+[HC(SO_2CF_3)_2]^-\cdot C_7H_8$ (**10**). The composition of this cationic Fe(II) complex follows from the ^{1}H NMR spectrum, which shows two diphos ligands ($\delta(CH_2)$ 2.1), one $HC(SO_2CF_3)_2^-$ ion (δ 3.9), and a quintet of unit area at δ −12.9 with J_{PH} = 48 Hz along with a broad resonance at δ −8.4 (2 H). The ^{1}H NMR spectrum agrees well with that recently reported for the crystallographically characterized $(diphos)_2FeH_3^+$ ion.[14] The ^{31}P{^{1}H} NMR spectrum is invariant from −30 to −100 °C and comprises a singlet at δ 80.2.[15] Solid **10** reacts extremely slowly with

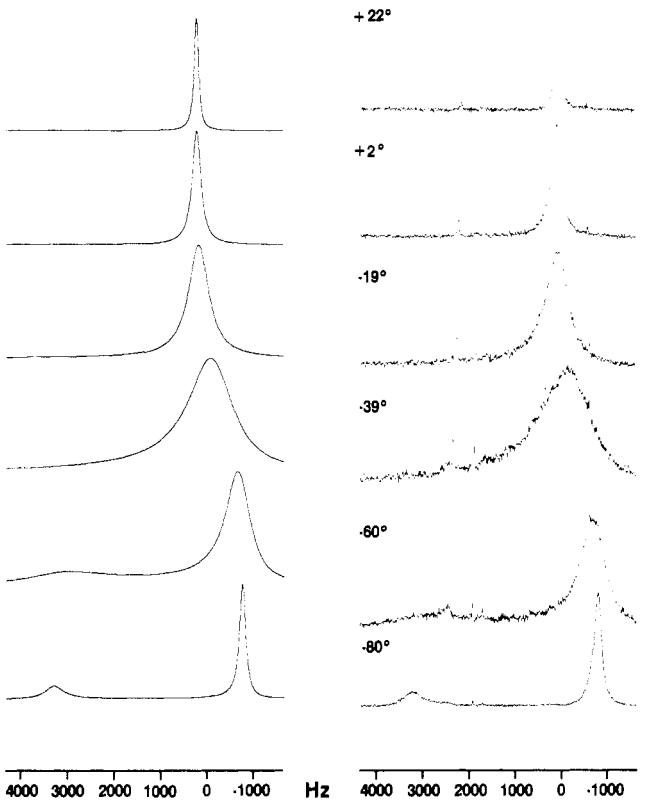

Figure 2. Calculated (left) and observed (right) ^{31}P DNMR spectra of $[(Ph_3P)_4OsH_3][HC(SO_2CF_3)_2]$ (**12**).

nitrogen; samples stored in a drybox under nitrogen contained ≤0.2% of this element after 2.5 years.

Derivatization of coordinatively unsaturated **10** is achieved in its reaction with trimethylphosphine to yield hydrogen and the 18-electron 1:1 adduct $[(diphos)_2FeHP(CH_3)_3]^+[HC(SO_2CF_3)_2]^-$ (**11**). The ^{31}P NMR spectrum of this material is diagnostic for octahedrally coordinated Fe(II) with trans, axial hydride and $(CH_3)_3P$ ligands. The diphos groups are chemically equivalent and give rise to a doublet of doublets, (δ 82.5, $J_{PP'}$ = 28 Hz, J_{PH} = 46 Hz) while the trimethylphosphine ligand gives rise to a doublet of quintets (δ −22.6, $J_{PP'}$ = 28 Hz, J_{PH} = 108 Hz). The structure of **11** is thus analogous to that of $[(C_2H_5O)_3P]_5RuH^+$, whose ^{31}P NMR spectrum was the AB_4 portion of an AB_4X pattern,[16] and to those of [1,2-bis(diethylphosphino)-ethane]$_2$FeHL$^+$ salts.[17,18]

Initial experiments involving the reaction of **1**–**3** with the osmium polyhydride $(Ph_3P)_3OsH_4$ did not yield tractable products although NMR analysis revealed the presence of a hydride species containing four triphenylphosphine ligands, indicating that some decomposition of the polyhydride to release Ph_3P had occurred. However, when $(Ph_3P)_3OsH_4$ in toluene is treated with 1 equiv each of $H_2C(SO_2CF_3)_2$ and Ph_3P, $[(Ph_3P)_4OsH_3]^+[HC(SO_2CF_3)_2]^-$ (**12**) separates in 42% yield. The ^{1}H NMR spectrum

(9) Emsley, J. W.; Feeney, J.; Sutcliffe, L. H. *High Resolution NMR Spectroscopy*; Pergamon: New York, NY., 1965; Chapter 8.
(10) Seddon, E. A.; Seddon, K. R. *The Chemistry of Ruthenium*, Elsevier: New York, NY, 1984; p 509.
(11) Dekleva, T. W.; Thorburn, I. S.; James, B. R. *Inorg. Chim. Acta* **1985**, *100*, 49.
(12) Jones, R. A.; Wilkinson, G.; Colquhoun, I. J.; McFarlane, W.; Galas, A. M. R.; Hursthouse, M. B. *J. Chem. Soc., Dalton Trans.* **1980**, 2480.
(13) Schumann, H.; Opitz, J. *J. Organomet. Chem.* **1980**, *186*, 91.
(14) Morris, R. H.; Sawyer, J. F.; Shiralian, M.; Zubkowski, J. D. *J. Am. Chem. Soc.* **1985**, *107*, 5581.
(15) (a) The cationic complex $[(diphos)_2Fe(\eta^2\text{-}H_2)H]^+$ is incorrectly formulated in ref 1. (b) The properties of **10** differ from those of $[(diphos)_2FeH]^+[BPh_4]^-$, prepared[18] by the reaction of $(diphos)_2FeHCl$ and $NaBPh_4$ in benzene, for which no NMR data are available. We have repeated this reaction and have obtained the prescribed blue product. It is, however, strongly paramagnetic and shows a broad EPR signal at g = 2.043; the estimated spin concentration, assuming a molecular weight of 1172, is at the 7 mol percent level. In addition, GC–MS analysis of the benzene filtrate discloses that biphenyl (0.02 mol/mol of Fe) is formed, presumably as a result of numinous electron-transfer processes; some $(diphos)_2FeH$ is formed as well. The ^{1}H NMR spectrum of this BPh_4 salt in CD_2Cl_2 exhibits a broad ($w/2$ = 1700 Hz) resonance at −18.2 ppm.
(16) Giannoccaro, P.; Sacco, A. *Inorg. Synth.* **1977**, *17*, 69.
(17) Harris, T. V.; Rathke, J. W.; Muetterties, E. L. *J. Am. Chem. Soc.* **1978**, *100*, 6966.
(18) Bancroft, G. M.; Mays, M. J.; Prater, B. E.; Stefanini, F. P. *J. Chem. Soc. A* **1970**, 2146.

of **12** demonstrates a binomial quintet at δ −9.83 ppm (J_{PH} = 19.6 Hz), indicating that the Os–H protons are equivalent at room temperature as are the triphenylphosphine groups [δ 6.96 (d, H_o), 6.84 (t, H_m), 7.29 (t, H_p)]. The $HC(SO_2CF_3)_2^-$ proton appears as a singlet at δ 3.89. Integration of the spectrum shows that the hydride:Ph_3P:$HC(SO_2CF_3)_2^-$ ratio is 3:4:1. The ambient-temperature $^{31}P\{^1H\}$ NMR spectrum comprises a broad singlet at δ 3.0; at 70 °C, decoupling of only the aromatic protons produces a 1:3:3:1 quartet, incompletely resolved owing to the 22-Hz ^{31}P line width, indicating the presence in **12** of three hydride ligands. The spin–lattice relaxation time, T_1, of the Os–H protons, measured at 9.4 T on a degassed 0.035 M solution of **12** in CD_2Cl_2, is 0.33 s at 22 °C and 1.3 s at −80 °C. These long relaxation times are indicative of an $Os(\eta^1\text{-}H)_3$ moiety. The dependence of T_1 on temperature suggests that it is determined mainly by spin rotation interactions rather than by dipolar contributions as has been reported for molecular hydrogen complexes.[19]

The $^{31}P\{^1H\}$ NMR spectrum of **12** in CD_2Cl_2 at −80 °C shows two singlets in a 3:1 ratio at δ −9.4 and 40.7. As the temperature increases, they coalesce in a manner typical of a dynamic NMR exchange process between sites of 3:1 relative populations. Spectra were calculated with the equations of Gutowsky and Holm for two sites of unequal populations undergoing exchange.[20] The observed and calculated ^{31}P NMR spectra are shown in Figure 2. The free energy of activation for the exchange process, ΔG^*, was calculated from absolute reaction rate theory: $1/\tau = (kT/h)\exp(-\Delta G^*/RT)$ where τ is the lifetime of any of the four triphenylphosphines with respect to interchange between two distinguishable sites. The linear temperature dependence of ΔG^*, from 8.32 kcal/mol at −80 °C to 9.93 kcal/mol at 22 °C, gives $\Delta H^* = 5.3 \pm 0.3$ kcal/mol and $\Delta S^* = -16 \pm 1$ eu. The quintet observed for the hydride protons in the ^1H NMR spectrum collapses (at about −60 °C) as the temperature is lowered, but the sample freezes before any multiplet structure is reestablished.

That two ^{31}P resonances in a 3:1 ratio are observed in the limiting low-temperature NMR spectrum of $(Ph_3P)_4OsH_3^+$ suggests that the phosphine and hydride ligands are arranged about the central osmium atom to form a capped octahedral coordination geometry. In an alternative view of the capped octahedron, four triphenylphospine ligands occupy the vertices of an osmium-centered tetrahedron. If the three hydrides lie on or near three of the four triangular faces of this tetrahedron, then two types of phosphorus environments in the observed 3:1 ratio would result. This is consistent with the solid-state structure of **12** (vide infra). Seven-coordinate complexes with all unidentate ligands should be stereochemically nonrigid,[21] but slow-exchange spectra of such materials are infrequently observed. Recent examples include $CrH_2[P(OMe)_3]_5$, rearrangements in which have been the subject of a detailed mechanistic analysis,[22] and $(PhPMe_2)_3OsH_4$.[23] The intramolecular process in $(Ph_3P)_4OsH_3^+$ that permutes ^1H and ^{31}P sites may well be similar to the tetrahedral jump mechanism elucidated in a classic crystallographic and DNMR study of six- and eight-coordinate H_2ML_4 and H_4ML_4 compounds.[24,25]

The polyhydrides $(phosphine)_3OsH_4$ are themselves fluxional.[23] That these materials undergo acid-catalyzed H–D exchange with C_2H_5OD led to the plausible suggestion that $(phosphine)_3OsH_5^+$ species are involved as intermediates.[26] Attempts to isolate the cationic pentahydrides as Ph_4B^- salts produced oils that evolved hydrogen on standing, but an analogue of **12**, $(PhPEt_2)_4OsH_3^+$, has been reported to form in the reaction of $(PhPEt_2)_4OsH_2$ with hydrogen chloride in refluxing benzene–methanol.[27] The reaction of $(PhPMe_2)_3OsH_4$ with $HBF_4{\cdot}OEt_2$ in acetonitrile proceeds in stepwise fashion by preequilibrium loss of dihydrogen and interception of the intermediates by acetonitrile to give $(PhPMe_2)_3OsH_5^+$, $(PhPMe_2)_3OsH_3(CH_3CN)^+$, *mer,cis*-$(PhPMe_2)_3OsH(CH_3CN)_2^+$, and *mer*-$(PhPMe_2)_3Os(CH_3CN)_3^{2+}$.[28] The molybdenum polyhydride $(Ph_2PMe)_4MoH_4$ evidently undergoes protonation by HBF_4 in methanol to form at low temperatures hydrogen and $(Ph_2PMe)_4MoH_3^+$,[29] but at room temperature, $[((Ph_2PMe)_3MoH_2)_2(\mu\text{-}F)_3]BF_4$ results;[30] the cationic pentahydride $(Ph_2PMe)_4WH_5^+$ may be stable. Although these high-coordinate, cationic polyhydrides are presumably fluxional, detailed analyses of the rearrangement mechanisms are not available. The importance of solvent effects in protonation of transition-metal hydrides is further exemplified by the reaction of $HBF_4{\cdot}Et_2O$ with $(PhPMe_2)_4MoH_4$ in acetonitrile, which produces a solvate, $(PhPMe_2)_4MoH_2(CH_3CN)_2^+$.[31]

Having established the solution-phase dynamic properties of $(Ph_3P)_4OsH_3^+$, a single-crystal X-ray study of its $HC(SO_2CF_3)_2^-$ salt was carried out to determine its solid-state structure.

Solid-State Structure of $[(Ph_3P)_4OsH_3]^+[HC(SO_2CF_3)_2]^-$. The crystal structure of **12** was determined at −90 °C and consists of well-separated cations and anions. A view of the osmium coordination core, including important distances and angles, is shown in Figure 3. Table III contains a more complete listing of metrical

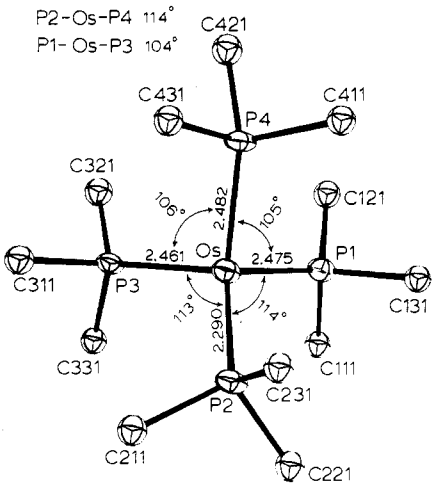

Figure 3. ORTEP view of the osmium coordination core in $[(Ph_3P)_4OsH_3][HC(SO_2CF_3)_2]$ (**12**) with important bond distances and angles. Ellipsoids are drawn with 50% probability boundaries.

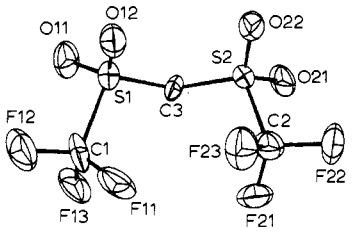

Figure 4. ORTEP view of the $HC(SO_2CF_3)_2^-$ ion in **12**. Ellipsoids are drawn with 50% probability boundaries.

(19) Crabtree, R. H.; Lavin, M. *J. Chem. Soc., Chem. Commun.* **1985**, 1661.
(20) Gutowsky, H. S.; Holm, C. H. *J. Chem. Phys.* **1956**, *25*, 1228.
(21) Jesson, J. P.; Muetterties, E. L. In *Dynamic Nuclear Magnetic Resonance Spectroscopy*; Jackman, L. M., Cotton, F. A., Eds.; Academic: New York, NY, 1975; p 289.
(22) Van Catledge, F. A.; Itel, S. D.; Jesson, J. P. *Organometallics* **1985**, *4*, 18.
(23) Green, M. A.; Huffman, J. C.; Caulton, K. G. *J. Organomet. Chem.* **1983**, *243*, C78. The low-temperature ^1H and ^{31}P NMR data in footnote 5 of this reference are consistent with a pentagonal-bipyramidal geometry in solution with two axial and one equatorial phosphine ligands, as occurs in the solid.
(24) Meakin, P.; Muetterties, E. L.; Jesson, J. P *J. Am. Chem. Soc.* **1973**, *95*, 75.
(25) Meakin, P.; Guggenberger, L. J.; Peet, W. G.; Muetterties, E. L.; Jesson, J. P. *J. Am. Chem. Soc.* **1973**, *95*, 1467.
(26) Douglas, P. G.; Shaw, B. L. *J. Chem. Soc. A* **1970**, 334.
(27) Bell, B.; Chatt, J.; Leigh, G. J. *J. Chem. Soc., Dalton Trans.* **1973**, 997. The number of hydride ligands in this cation is not rigorously established.
(28) Bruno, J. W.; Huffman, J. C.; Caulton, K. G. *J. Am. Chem. Soc.* **1984**, *106*, 1663.
(29) Carmona-Guzman, E.; Wilkinson, G. *J. Chem. Soc., Dalton Trans.* **1977**, 1716.
(30) Crabtree, R. H.; Hlatky, G. G.; Holt, E. M. *J. Am. Chem. Soc.* **1983**, *105*, 7302.
(31) Rhodes, L. F.; Zubkowski, J. D.; Folting, K.; Huffman, J. C.; Caulton, K. G. *Inorg. Chem.* **1982**, *21*, 4185.

Table I. Summary of Crystal Data and Intensity Collection for $[(Ph_3P)_4OsH_3]^+[HC(SO_2CF_3)_2]^-$

Crystal Parameters	
cryst syst	monoclinic
space group	$P2_1/n$
cell params (−90 °C; +25 °C)	
a, Å	14.122 (6); 14.192 (3)
b, Å	13.636 (1); 13.758 (5)
c, Å	33.646 (2); 33.927 (7)
α, deg	90; 90
β, deg	90.90 (4); 90.80 (4)
γ, deg	90; 90
V, Å^3	6478 (5); 6624 (5)
Z	4
calcd density, g cm^{-3}	1.557
abs coeff, cm^{-1}	21.96
cryst dimens, mm	0.25 × 0.20 × 0.15
max, min, av transmissn factors	1.0, 0.73, 0.90
formula	$OsS_2P_4F_6O_4C_{75}H_{61}$
fw	1588.5
Measurement of Intensity Data	
diffractometer	CAD 4
radiation (λ, Å)	Mo Kα (0.710 69)
Graphite Monochromatized	
scan range 2θ, deg	0–51
no. of unique reflcns measd (region)	11 777 ($+h,+k,\pm l$)
no. of obsd reflcns[a]	7188 [$F_o^2 > 2\sigma(F_o^2)$]
refinement by full-matrix least-squares	
no. of params	470
R[b]	0.095
R_w[b]	0.099
GOF[b]	2.45
p[a]	0.04

[a] The intensity data were processed as described in: *CAD4 and SDP User's Manual*; Enraf-Nonius: Delft, Holland, 1978. The net intensity $I = [K/(NPI)](C - 2B)$, where K = 20.1166 × attenuator factor, NPI = ratio of fastest possible scan rate to scan rate for the measurement, C = total count, and B = total background count. The standard deviation in the net intensity is given by $[\sigma(I)]^2 = (K/(NPI))^2[C + 4B + (pI)^2]$ where p is a factor used to downweight intense reflections. The observed structure factor amplitude F_o is given by $F_o = (I/Lp)^{1/2}$, wehre Lp = Lorentz and polarization factors. The $\sigma(I)$'s were converted to the estimated errors in the relative structure factors $\sigma(F_o)$ by $\sigma(F_o) = 1/2[\sigma(I)/I]F_o$. [b] The function minimized was $\sum w(|F_o| - |F_c|)^2$, where $w = 1/[\sigma(F_o)]^2$. The unweighted and weighted residuals are defined as $R = (\sum||F_o| - |F_c||)/\sum|F_o|$ and $R_w = [(\sum w(|F_o| - |F_c|))^2/(\sum w|F_o|)^2]^{1/2}$. The error in an observation of unit weight (GOF) is $[\sum(|F_o| - |F_c|)^2/(NO - NV)]^{1/2}$, where NO and NV are the numbers of observations and variables, respectively.

data. The OsP_4 unit shows a significant trigonal distortion along the Os–P_2 vector from idealized tetrahedral geometry. The Os–P_2 distance is short [2.290 (3)Å] while the other Os–P distances are similar and significantly longer [average 2.470 (3) Å]. The phosphorus atoms P1, P3, and P4 are bent away from P2 so that the P2–Os–P angles are large [average 113.6 (1)°] while the P–Os–P angles not involving P2 average 105.1 (1)°. This distortion is clearly due to the three hydride ligands that are considered to be positioned on the three triangular faces approximately trans to P1, P3, and P4.

The is entirely consistent with the solution-phase structure deduced from NMR data (vide supra). The hydride ligands were, predictably, not located in the X-ray analysis.[32] The average Os–P distance is 2.430 (3) Å and is somewhat longer than that in [*fac*-$(PhPMe_2)_3Os(CH_3CN)_3][PF_6]_2$, 2.327 (2) Å.[28] Significant lengthening of three of the four Os–P bonds is a result of a structural trans effect of the three hydride ligands. A similar effect has been observed in *mer*-$(Ph_3P)_3IrH_3$, in which the Ir–P bond trans to hydrogen is 0.061 Å longer than those cis to hydrogen.[33] In **12**, the OsP_4H_3 unit is describable as a distorted, capped octahedron, the cap being formed by P2. The coordination geometry thus differs from that of $(PhPMe_2)_3OsH_4$[34] and $(diphos)_2ReH_3$,[35] which adopt a distorted pentagonal form.

An ORTEP view of the $HC(SO_2CF_3)_2^-$ anion is shown in Figure 4. The distances and angles in it are very similar to those observed in the Rb^+ salt.[7]

Table II. Table of Positional Parameters and Their Estimated Standard Deviations[a]

atom	x	y	z	B, Å^2
Os	0.25800 (4)	0.24729 (6)	0.10604 (2)	1.843 (9)
P1	0.0949 (3)	0.2415 (4)	0.0781 (1)	1.90 (7)
P2	0.2704 (3)	0.1962 (3)	0.1707 (1)	1.83 (8)
P3	0.3070 (3)	0.4190 (3)	0.0972 (1)	1.83 (8)
P4	0.3553 (3)	0.1505 (3)	0.0594 (1)	1.79 (8)
C111	0.006 (1)	0.318 (1)	0.1035 (5)	2.0 (3)*
C121	0.070 (1)	0.272 (1)	0.0254 (5)	2.1 (3)*
C131	0.037 (1)	0.123 (1)	0.0822 (5)	1.8 (3)*
C211	0.348 (1)	0.271 (1)	0.2032 (4)	2.0 (3)*
C221	0.160 (1)	0.190 (1)	0.1996 (5)	2.0 (3)*
C231	0.319 (1)	0.072 (1)	0.1773 (5)	1.8 (3)*
C311	0.427 (1)	0.447 (1)	0.1135 (5)	2.0 (3)*
C321	0.300 (1)	0.479 (1)	0.479 (5)	2.2 (3)*
C331	0.241 (1)	0.509 (1)	0.1262 (5)	1.9 (3)*
C411	0.321 (1)	0.021 (1)	0.0545 (5)	1.8 (3)*
C421	0.368 (1)	0.185 (1)	0.0068 (5)	2.2 (3)*
C431	0.480 (1)	0.139 (1)	0.0740 (5)	1.8 (3)*
S1	0.6985 (3)	0.095 (4)	0.2594 (1)	3.0 (1)
S2	0.6632 (4)	0.2239 (3)	0.3287 (1)	2.9 (1)
O11	0.639 (1)	0.025 (1)	0.2383 (4)	4.4 (3)
O21	0.5793 (8)	0.265 (1)	0.3461 (3)	4.0 (3)
C3	0.631 (1)	0.170 (1)	0.2857 (7)	3.0 (4)
F22	0.7569 (8)	−0.1105 (8)	0.1490 (3)	4.6 (3)
F13	0.6729 (9)	0.204 (1)	0.1961 (3)	5.2 (3)
C1	0.741 (1)	0.169 (2)	0.2178 (5)	3.8 (5)
F11	0.7945 (7)	0.244 (1)	0.2307 (3)	4.9 (3)
F12	0.7980 (9)	0.116 (1)	0.1945 (3)	5.7 (3)
F21	0.6922 (9)	0.3882 (8)	0.2902 (3)	4.8 (3)
O12	0.7832 (9)	0.064 (1)	0.2800 (4)	3.8 (3)
O22	0.727 (1)	0.169 (1)	0.3535 (4)	4.6 (3)
C2	0.733 (1)	0.335 (1)	0.3179 (6)	3.5 (4)
F23	0.8189 (8)	0.3119 (9	0.3069 (3)	4.8 (3)

[a] Values denoted with an asterisk indicate that the atoms were refined isotropically. Anisotropically refined atoms are given in the form of the isotropic equivalent thermal parameter defined as $^4/_3[a^2B(1,1) + b^2B(2,2) + c^2B(3,3) + ab(\cos\gamma)B(1,2) + ac(\cos\beta)B(1,3) + bc(\cos\alpha)B(2,3)]$. The atoms are shown in Figures 3 and 4. Parameters of all atoms are in the supplementary material.

Experimental Section

Reactions were carried out, unless otherwise specified, under a water- and oxygen-free nitrogen atmosphere. Toluene and hexane were distilled from Na–K alloy; CD_2Cl_2 and C_6D_6 used as NMR solvents were stored under vacuum over CaH_2. Ethanol and dichloromethane used for conductance measurements were deoxygenated by purging with N_2 and stored under nitrogen over 4A molecular sieves. Fluorocarbon acids were prepared by the method of Koshar and Mitsch.[36] NMR spectra were obtained on a Varian XL-200 instrument at 200 (^{1}H) and 80.98 (^{31}P) MHz. Positive chemical shifts are downfield relative to internal $(CH_3)_4Si$ or $CFCl_3$ and external 85% H_3PO_4 references. In all cases, ^{31}P spectra were obtained both with white noise ^{1}H decoupling and with narrow band decoupling of the aromatic protons. NMR samples were prepared on a high-vacuum line and stored in liquid nitrogen. Infrared spectra were recorded on mulls prepared in a drybox by using Nujol that had been previously degassed and dried with molten sodium.

$[(Ph_3P)_3RuH(CO)][HC(SO_2CF_3)_2]\cdot 2C_7H_8$ (6). Toluene (12 mL) was added to a mixture of 0.54 g (0.6 mmol) of $(Ph_3P)_3RuH_2(CO)$ and 0.17

(32) Crystallographic studies of transition-metal hydrides have been thoroughly reviewed: Teller, R. S.; Bau, R. *Struct. Bonding (Berlin)* **1981**, *44*, 1.

(33) Clark, G. R.; Skelton, B. W.; Waters, T. N. *Inorg. Chim.* Acta **1975**, *12*, 235.

(34) Hart, D. W.; Bau, R.; Koetzle, T. F. *J. Am. Chem. Soc.* **1977**, *99*, 775. Hydride positions in this compound were accurately located by neutron diffraction techniques.

(35) Albano, V.; Bellon, P. *J. Organomet. Chem.* **1972**, *37*, 151.

(36) Koshar, R. J.; Mitsch, R. A. *J. Org. Chem.* **1973**, *38*, 3358.

Table III. Selected Distances and Angles and Their Esd's for $[(Ph_3P)_4OsH_3][HC(SO_2CF_3)_2]$

		Distances, Å			
Os–P1	2.475 (3)	P2–C211	1.84 (1)	P4–C411	1.84 (1)
Os–P2	2.290 (3)	P2–C221	1.85 (1)	P4–C421	1.84 (1)
Os–P3	2.461 (3)	P2–C231	1.84 (1)	P4–C431	1.83 (1)
Os–P4	2.482 (3)	P3–C311	1.81	81–011	1.45 (1)
P1–C111	1.85 (1)	P3–C321	1.85 (1)	S1–O12	1.44 (1)
P1–C121	1.85 (1)	P3–C331	1.84 (1)	S1–C1	1.83 (1)
P1–C131	1.82 (1)	C2–F21	1.31 (2)	S1–C3	1.66 (1)
C1–F11	1.34 (2)	C2–F22	1.35 (2)	S2–O21	1.45 (1)
C1–F12	1.35 (2)	C2–F23	1.32 (2)	S2–O22	1.43 (1)
C1–F13	1.29 (2)			S2–C2	1.84 (1)
				S2–C3	1.68 (1)
		Angles, deg			
P1–Os–P2	114.1 (1)	Os–P1–C111	116.3 (3)	Os–P3–C311	115.5 (3)
P1–Os–P3	104.3 (1)	Os–P1–C121	121.0 (3)	Os–P3–C321	121.3 (3)
P1–Os–P4	105.4 (1)	Os–P1–C131	114.6 (3)	Os–P3–C331	115.3 (3)
P2–Os–P3	112.8 (1)	Os–P2–C211	115.7 (3)	Os–P4–C411	114.8 (3)
P2–Os–P4	113.8 (1)	Os–P2–C221	117.5 (3)	Os–P4–C421	122.1 (3)
P3–Os–P4	105.7 (1)	Os–P2–C231	114.6 (3)	Os–P4–C431	114.6 (3)
S1–C3–S2	125.5 (8)	C3–S2–O21	108.0 (6)	S1–C1–F11	111 (1)
C3–S1–O11	109.6 (6)	C3–S2–O22	115.8 (6)	S1–C1–F12	111 (1)
C3–S1–O12	113.7 (6)	C3–S2–C2	109.0 (6)	S1–C1–F13	113 (1)
C3–S1–C1	105.2 (6)	O21–S2–O22	118.7 (6)	S2–C2–F21	112 (1)
O11–S1–O12	121.0 (6)	O21–S2–C2	101.6 (6)	S2–C2–F22	111 (1)
O11–S1–C1	100.6 (6)	O22–S2–C2	102.3 (6)	S2–C2–F23	109 (1)
O21–S1–C1	104.5 (6)				

g (0.6 mmol) of $H_2C(SO_2CF_3)_2$. The reaction mixture was stirred at room temperature for 6 h, during which time the starting hydride dissolved and was replaced by a light yellow crystalline solid. The product was isolated by filtration in a drybox, washed with fresh toluene, and vacuum-dried to yield 0.5 g (73%) of **6**. Anal. Calcd for $C_{72}H_{63}F_6O_5P_3RuS_2$: C, 62.0; H, 4.7; P, 6.9; Ru, 7.1; S, 4.6. Found: C, 62.6; H, 4.6; P, 6.7; Ru, 7.3; S, 4.6.

$[(Ph_3P)_3RuH(CO)][HC(SO_2C_8F_{17})_2]$ (6a) was similarly prepared from $H_2C(SO_2C_8F_{17})_2$. It was precipitated from toluene with hexane. Anal. Calcd for $C_{86}H_{63}F_{34}O_5P_3RuS_2$: C, 49.6; H, 3.0. Found: C, 49.2; H, 2.9. IR: 1990, 1945 cm^{-1}. NMR (C_6D_6): ^1H, δ 3.86, −6.6 (dt, 103, 25); ^{13}C, δ 64.2 ($^1J_{CH}$ = 184 Hz, $^3J_{CF}$ = 16 Hz), 207.0 (CO).

$[(Ph_3P)_3OsH(CO)][HC(SO_2CF_3)_2]\cdot C_7H_8$ (7). Toluene (12 mL) was added to 0.5 g of $(Ph_3P)_3OsH_2(CO)$ and 0.14 g of **1**. After being stirred for 24 h, the reaction mixture was filtered in a drybox to remove a small amount of insoluble solids. Dilution of the filtrate with 4 mL of hexane caused the product to separate as white microcrystals, which were collected on a frit and vacuum-dried. The yield was 0.6 g (82%). Anal. Calcd for $C_{72}H_{43}F_6O_5OsP_3S_2$: C, 59.3; H, 4.3; Os, 13.0; P, 6.4; S, 4.4. Found: C, 59.4; H, 4.5; Os, 12.9; P, 6.0; S, 4.1.

$[(Ph_3P)_4Ru_2(CO)_2(\mu\text{-}Cl)_2(\mu\text{-}H)][BPh_4]$ (8). A mixture of 0.95 g of $(Ph_3P)_3Ru(CO)Cl$, 0.29 g (1.04 mmol) of $H_2C(SO_2CF_3)_2$, and 17 mL of toluene was stirred and heated for 16 h with a 70 °C oil bath. The oil that separated was triturated with hexane to give a yellow solid. This was extracted with 10 mL of warm ethanol and filtered to remove 0.20 g of the insoluble ruthenium starting material. On addition of 0.3 g of $NaBPh_4$ in 3 mL of ethanol to the filtrate, **8** separated as a yellow microcrystalline powder. It was collected on a frit, washed with ethanol, and then vacuum-dried to give 0.28 g of product (42% based on starting material consumed). Anal. Calcd for $C_{98}H_{81}BCl_2O_2P_4Ru_2$: C, 69.3; H, 4.8; Cl, 4.2; P, 7.3; Ru, 11.9. Found: C, 69.1; H, 4.7; Cl, 4.0; P, 7.5; Ru, 12.2.

$[(diphos)_2FeCl][HC(SO_2CF_3)_2]$ (9). Toluene (20 mL) was added by vacuum transfer to 0.88 g (1 mmol) of $(diphos)_2FeHCl$ and 0.28 g (1 mmol) of **1**. On warming to room temperature, hydrogen evolution occurred and the starting material was replaced by a yellow, microcrystalline phase. This was isolated by filtration, washed with more solvent, and vacuum-dried to give 1.0 g (86%) of product. Anal. Calcd for $C_{55}H_{46}ClF_6FeS_2O_4P_4$: C, 56.6; H, 4.2; Cl, 3.0; Fe, 4.8; P, 10.6; S, 5.5. Found: C, 57.1; H, 4.2; Cl, 3.4; Fe, 4.7; P, 10.3; S, 5.3.

$[(diphos)_2Fe(\eta^2\text{-}H_2)H][HC(SO_2CF_3)_2]\cdot C_7H_8$ (10). On a high vacuum line, 8 mL of toluene was condensed onto 0.30 g (0.3 mmol) of $(diphos)_2FeH_2\cdot 2C_7H_8$ and 0.084 g (0.3 mmol) of $H_2C(SO_2CF_3)_2$. After warming to room temperature, the flask was wrapped with aluminum foil. The contents were stirred for 16 h and then filtered in a drybox. The yield of yellow, powdery product, after filtration, washing with fresh solvent, and vacuum-drying, was 0.32 g (71%). Anal. *Calcd* for $C_{62}H_{61}F_6O_4P_4S_2$: C, 60.7; H, 4.9; F, 9.3; Fe, 4.6; N, 0.0; P, 10.1; S, 5.2. Found: C, 61.4; H, 5.1; F, 9.6; Fe, 4.8; N, <0.2; P, 9.8; S, 5.5. This compound is readily decomposed by air.

$[(diphos)_2FeHP(CH_3)_3][HC(SO_2CF_3)_2]$ (11). Trimethylphosphine (0.12 mmol) was condensed onto a frozen solution of 0.12 g (0.1 mmol) of **10** in 5 mL of dry, degassed dichloromethane. after the mixture was warmed to room temperature and stirred for 2 h, volatiles were pumped off and the residue was recrystallized in a drybox from dichloromethane–hexane to provide 0.1 g (83%) of **11** as an orange powder. Anal. Calcd for $C_{58}H_{59}F_6FeO_4P_5S_6$: C, 57.6; H, 4.9; Fe, 4.6; P, 12.9. Found: C, 58.0; H, 4.9; Fe, 4.5; P, 12.6.

$[(Ph_3P)_4OsH_3][HC(SO_2CF_3)_2]$ (12). A mixture of 10 mL of toluene, 0.09 g of triphenylphosphine, 0.33 g of $(Ph_3P)_3OsH_4$, and 0.09 g of $H_2C(SO_2CF_3)_2$ (0.33 mmol of each reactant) was stirred at room temperature for 24 h and then heated at 65 °C for 24 h. In a drybox, the light gray solid phase was collected on a filter, washed with toluene, and recrystallized from dichloromethane–ethanol to give 0.22 g (43%) of colorless **12**. Anal. Calcd for $C_{75}H_{64}F_6O_4OsP_4S_2$: C, 58.8; H, 4.2; F, 7.5; Os, 12.4; P, 8.8; S, 4.2. Found: C, 59.2; H, 4.3; F, 7.5; Os, 12.7; P, 9.1; S, 4.0. IR: ν_{OsH} 2118, 2128 cm^{-1} (Nujol); 2106 cm^{-1} (CH_2Cl_2). Conductance (1×10^{-3} M in CH_2Cl_2): 39 Ω^{-1} cm^2 mol^{-1}. Crystals used for X-ray diffraction experiments were grown by slow diffusion under nitrogen of methanol into a dichloromethane solution of **12**.

DNMR Spectra. The variable-temperature ^{31}P DNMR spectra were recorded using gated ^1H decoupling with a 10% duty cycle in order to minimize RF heating of the sample. They were recorded with a 0.1-s acquisition time, 1.0-s delay, and 20-μs (40°) pulses. The spectrometer thermistor was calibrated by substituting a neat methanol sample for the analytical sample. The spin decoupler coil was used to observe the ^1H resonance, and temperatures were determined from the calibration curve of Van Geet.[37] Resonances for the two different types of phosphorus were observable between −80 and −110 °C. The difference in chemical shifts showed a significant dependence on temperature, 0.8 Hz deg^{-1}, but this is insignificant compared to the 4000-Hz frequency separation of the two peaks. Corrections for P–P coupling or line width in the absence of exchange were also not significant because of the large line widths, which varied from 110 Hz at 22 °C to a maximum of 1300 Hz at the coalescence temperature (ca. −40 °C) to 190 Hz at −80 °C. Lifetimes were calculated from the equations of Gutowsky and Holm[20] to simulate the spectra. The calculations were performed with an iterative Apple II(+) microcomputer program.[38] Errors of ±0.3 kcal/mol in ΔH^* and ±1 eu in ΔS^* were calculated by following the procedure described by Newmark et al.[39] but assuming a maximum systematic error of ±2 °C in the temperature. These errors are small because the chemical shift difference between the two exchanging sites exceeds 4000 Hz.

Collection and Reduction of X-ray Data. A summary of crystal and intensity data is presented in Table I. A crystal of $[(Ph_3P)_4OsH_3][HC-$

(37) van Geet, A. L. *Anal. Chem.* **1971**, *43*, 679.
(38) Newmark, R. A. *J. Chem. Educ.* **1983**, *60*, 45.
(39) Siedle, A. R.; Newmark, R. A.; Kruger, A. A.; Pignolet, L. H. *Inorg. Chem.* **1981**, *20*, 3399.

$(SO_2CF_3)_2$] was secured to the end of a glass fiber with 5-min epoxy resin. The crystal was maintained at −90 ± 1 °C during lineup and data collection. The crystal was found to belong to the monoclinic crystal class by the Enraf-Nonius CAD 4-SDP peak search, centering, and indexing programs.[40] Background counts were measured at both ends of the scan range with use of an ω–2θ scan, equal, at each side, to one fourth of the scan range of the peak. In this manner, the total duration of background measurements is equal to half of the time required for the peak scan. The intensities of three standard reflections were measured every 1.5 h of X-ray exposure, and no decay was noted. The data were corrected for Lorentz, polarization, and background effects and for the effects of absorption (μ = 22.0 cm^{-1}). An empirical absorption correction was applied by using the SDP program EAC.[39]

Solution and Refinement of the Structure. The structure was solved by conventional heavy-atom techniques. The Os atom was located by Patterson synthesis. Full-matrix least-squares refinement and difference-Fourier calculations were used to locate all the remaining hydrogen atoms. The atomic scattering factors were taken from the usual tabulation,[41] and the effects of anomalous dispersion were included in F_c by using Cromer and Ibers'[42] values of $\Delta f'$ and $\Delta f''$. In the final least-squares cycle, the largest parameter shift was 0.05 times its esd. The final difference-Fourier map did not reveal significant residual electron density except in the region approximately 1 Å from the Os atom. The highest peak in this region was 5 e $Å^{-3}$. Phenyl hydrogen atom positions were calculated (d_{C-H} set at 0.95 Å) and included in structure factor calculations but were not refined. The final positional and thermal parameters of the refined atoms appear in Table II and as supplementary material. The labeling scheme for the cation is presented in Figure S1. A table of observed and calculated structure factors is available as supplementary material.

The y coordinate of the Os atom is near $^1/_4$ so that the Os atoms are pseudo-B-centered. Since they dominate the scattering, this means that the entire structure appears to be pseudo-B-centered; that is, the $h + l$ odd reflections are all weak. The data set used, $F_o^2 \geq 2\sigma(F_o^2)$, gave an overall R = 0.095 with R = 0.084 for the $h + l$ even reflections and only R = 0.134 for the $h + l$ odd reflections only. Had we used the data set with $F_o^2 \geq 3\sigma(F_o^2)$, the overall R would have been 0.064, but this would have arisen by cutting out most of the $h + l$ odd reflections, which is inappropriate. The distances, angles, and least-squares planes within the phenyl rings (see supplementary material) are in good agreement with the expected values, which provides a good check on the quality of the structure.

Acknowledgment. We are grateful to members of the 3M Analytical and Properties Research Laboratory for the spectroscopic and analytical data and to Robert Koshar, 3M Industrial and Consumer Sector Research Laboratory, for gifts of fluorocarobn acids. L.H.P. also acknowledges support by the National Science Foundation of his contribution to this work.

Registry No. **6**, 88825-79-0; **6a**, 103530-21-8; **7**, 88825-81-4; **8**, 103439-64-1; **9**, 103439-75-4; **10**, 103439-66-3; **11**, 103439-68-5; **12**, 88841-59-2; $(Ph_3P)_3RuH_2(CO)$, 25360-32-1; $(Ph_3P)_3OsH_2(CO)$, 12104-84-6; $(Ph_3P)_3Ru(CO)Cl$, 103439-70-9; $(diphos)_2FeH_2$, 47898-23-7; $(Ph_3P)_3OsH_4$, 24228-59-9; $(diphos)_2FeHCl$, 32490-70-3.

Supplementary Material Available: Figure S1, an ORTEP view of the cation in **12** showing the labeling scheme, and tables of positional parameters and their estimated deviations, general temperature factor expressions, weighted least-squares planes, torsion angles, and distances and angles within phenyl rings in **12** (18 pages); a table of observed and calculated structure factor amplitudes (31 pages). Ordering information is given on any current masthead page.

(40) All calculations were carried out on PDP 8A and 11/34 computers with use of the Enraf-Nonius CAD 4-SDP programs. This crystallographic computing package is described: Frenz, B. A. In *Computing in Crystallography*; Shenk, H., Olthof-Hazekamp, R., van Konigsveld, H., Bassi, G. C., Eds.; Delft University Press: Delft, Holland, 1978; pp 64–71. *CAD 4 and SDP User's Manual*; Enraf-Nonius: Delft, Holland, 1978.
(41) Cromer, D. T.; Waber, J. T. *International Tables for X-Ray Crystallography*; Kynoch: Birmingham, England, 1974; Vol. IV, Table 2.2.4. Cromer, D. T. *Ibid.* Table 2.3.1.
(42) Cromer, D. T.; Ibers, J. A. In ref 38.

Contribution from the Department of Chemistry, University of South Carolina, Columbia, South Carolina 29208

Ligand Substitution vs. Ligand Addition. 1. Differences in Reactivity between First- and Third-Row Transition-Metal Clusters. Reactions of Dimethylamine with the Sulfidometal Carbonyl Clusters $M_3(CO)_9(\mu_3\text{-}S)_2$ (M = Fe, Os)

Richard D. Adams* and James E. Babin

Received February 24, 1986

The reactions of the cluster complexes $M_3(CO)_9(\mu_3\text{-}S)_2$ (**1**, M = Fe; **3**, M = Os) with dimethylamine follow decidedly different pathways. The reaction with **1** yields the substitution product $Fe_3(CO)_8(Me_2NH)(\mu_3\text{-}S)_2$ (**2**) in 66% yield while the reaction with **3** yields the addition product $Os_3(CO)_8(\mu_3\text{-}S)_2(\mu\text{-}Me_2NC{=}O)(\mu\text{-}H)$ (**4**) in 93% yield. Both products have been characterized by IR and ^1H NMR spectroscopies and single-crystal X-ray diffraction analyses. For **2**, space group $P2_1/c$, a = 7.004 (1) Å, b = 13.652 (2) Å, c = 17.764 (2) Å, β = 91.87 (1)°, Z = 4, and ρ_{calcd} = 1.96 g/cm^3. The structure was solved by direct methods and was refined (1549 reflections) to the final values for the residuals R = 0.0437 and R_w = 0.0483. For **4**, space group $P2_1/c$, a = 9.223 (2) Å, b = 10.599 (4) Å, c = 19.773 (3) Å, β = 91.881 (16)°, Z = 4, and ρ_{calcd} = 3.20 g/cm^3. The structure was solved by direct methods and was refined (2485 reflections) to the final values of the residuals R = 0.0499 and R_w = 0.0583. The structure of **2** consists of an open triangular cluster of three iron atoms with two iron–iron bonds. There are triply bridging sulfido ligands on each side of the Fe_3 plane and a Me_2NH ligand positioned trans to one of the sulfido ligands on one of the external iron atoms. The structure of **4** consists of an open cluster having only one osmium–osmium bond, and it contains a bridging hydride ligand. There are two triply bridging sulfido ligands and a C,O-bonded bridging dimethylcarbamoyl ligand.

Introduction

Studies of the chemistry of transition-metal cluster compounds have revealed a variety of new and unusual ligand[1] and cluster[2] transformations. However, relatively few studies have been focused on the comparative reactivity of an homologous series of cluster compounds.[3] One of the good examples of such a study is that on the substitutional behavior of the tetranuclear clusters $M_4(CO)_{12}$ (M = Co, Rh, Ir) by phosphine and phosphite ligands.[3]

(1) Adams, R. D.; Horvath, I. T. *Prog. Inorg. Chem.* **1985**, *33*, 127.
(2) Vahrenkamp, H. *Adv. Organomet. Chem.* **1983**, *22*, 169.
(3) Muetterties, E. L.; Burch, R. R.; Stolzenberg, A. M. *Annu. Rev. Phys. Chem.* **1982**, *33*, 89 and references therein.

0020-1669/86/1325-3418$01.50/0